Research Article Open Access

Yoji Arakawa*, Daisuke Endo, Kei Ikehata, Junya Oshika, Taro Shinmura, and Yasushi Mori

Two types of gabbroic xenoliths from rhyolite dominated Niijima volcano, northern part of Izu-Bonin arc: petrological and geochemical constraints

DOI 10.1515/geo-2017-0001
Received Jan 27, 2016; accepted Jun 15, 2016

Abstract: We examined the petrography, petrology, and geochemistry of two types of gabbroic xenoliths (A- and B-type xenoliths) in olivine basalt and biotite rhyolite units among the dominantly rhyolitic rocks in Niijima volcano, northern Izu-Bonin volcanic arc, central Japan. A-type gabbroic xenoliths consisting of plagioclase, clinopyroxene, and orthopyroxene with an adcumulate texture were found in both olivine basalt and biotite rhyolite units, and B-type gabbroic xenoliths consisting of plagioclase and amphibole with an orthocumulate texture were found only in biotite rhyolite units. Geothermal- and barometric-modelling based on mineral chemistry indicated that the A-type gabbro formed at higher temperatures (899-955°C) and pressures (3.6-5.9 kbar) than the B-type gabbro (687-824°C and 0.8-3.6 kbar). These findings and whole-rock chemistry suggest different parental magmas for the two types of gabbro. The A-type gabbro was likely formed from basaltic magma, whereas the B-type gabbro was likely formed from an intermediate (andesitic) magma. The gabbroic xenoliths in erupted products at Niijima volcano indicate the presence of mafic to intermediate cumulate bodies of different origins at relatively shallower levels beneath the dominantly rhyolitic volcano.

Keywords: Gabbroic xenolith; Niijima volcano; Cumulate; Crystal fractionation

1 Introduction

Mafic xenoliths in volcanic rocks can provide valuable information about the petrology and chemistry of unexposed subvolcanic basement, the composition of parental mafic magmas and differentiation processes during the early stage of magmatic evolution [*e.g.* 1–5]. Most of the mafic xenoliths in volcanic rocks from island arc systems fall into one of three categories: cognate xenoliths that are indicative of magma mixing [*e.g.* 6, 7], plutonic blocks derived from middle to lower crustal sources [*e.g.* 8, 9], or cumulate rocks formed by crystallization and precipitation in magma reservoirs [*e.g.* 10–12]. Among these, rare gabbroic xenoliths are found in rocks extruded from dominantly felsic (dacite to rhyolite) volcanoes (*e.g.* Mount St. Helens, Washington [13, 14]; Little Glass Mountain, California [15]).

Niijima volcano in the northern Izu-Bonin volcanic arc is a rare example of a volcano that has produced predominantly rhyolitic lava domes and pyroclastic rocks accompanied by only minor andesitic to basaltic flow. Its volcanic products contain various types of xenolith [*e.g.* 16], but include both volcanic xenoliths (andesitic to basaltic composition) in rhyolitic pyroclastic flow deposits and lavas [*e.g.* 16], and plutonic xenoliths (*e.g.* diorite, tonalite, and gabbro) in basaltic basal surge deposits and rhyolitic units [*e.g.* 16, 17]. However, there are few published discussions of the origin and process of formation of these types of xenolith and their relationships with erupting host magmas. In this paper, we present the results of new petrographical, petrological, and chemical investigations of the two types of gabbroic xenoliths found at Niijima, discuss the processes and temperature-pressure conditions of their formation, and consider possible parental mag-

***Corresponding Author: Yoji Arakawa:** Faculty of Life and Environmental Sciences, University of Tsukuba, 1-1-1 Tennodai, Tsukuba, Ibaraki 305-8572, Japan; Email: yaraka@geol.tsukuba.ac.jp
Daisuke Endo, Kei Ikehata: Faculty of Life and Environmental Sciences, University of Tsukuba, 1-1-1 Tennodai, Tsukuba, Ibaraki 305-8572, Japan
Junya Oshika: Japan Oil, Gas and Metal National Corporation, 2-10-1 Toranomon, Minato-ku, Tokyo 105-0001, Japan
Taro Shinmura: Faculty of Economics, Kumamoto-Gakuen University, 2-5-1 Oe, Kumamoto, Kumamoto 862-8680, Japan
Yasushi Mori: Kitakyushu Museum of Natural History and Human History, 2-41 Yahatahigashi, Higashida, Kitakyushu, Fukuoka 805-0071, Japan

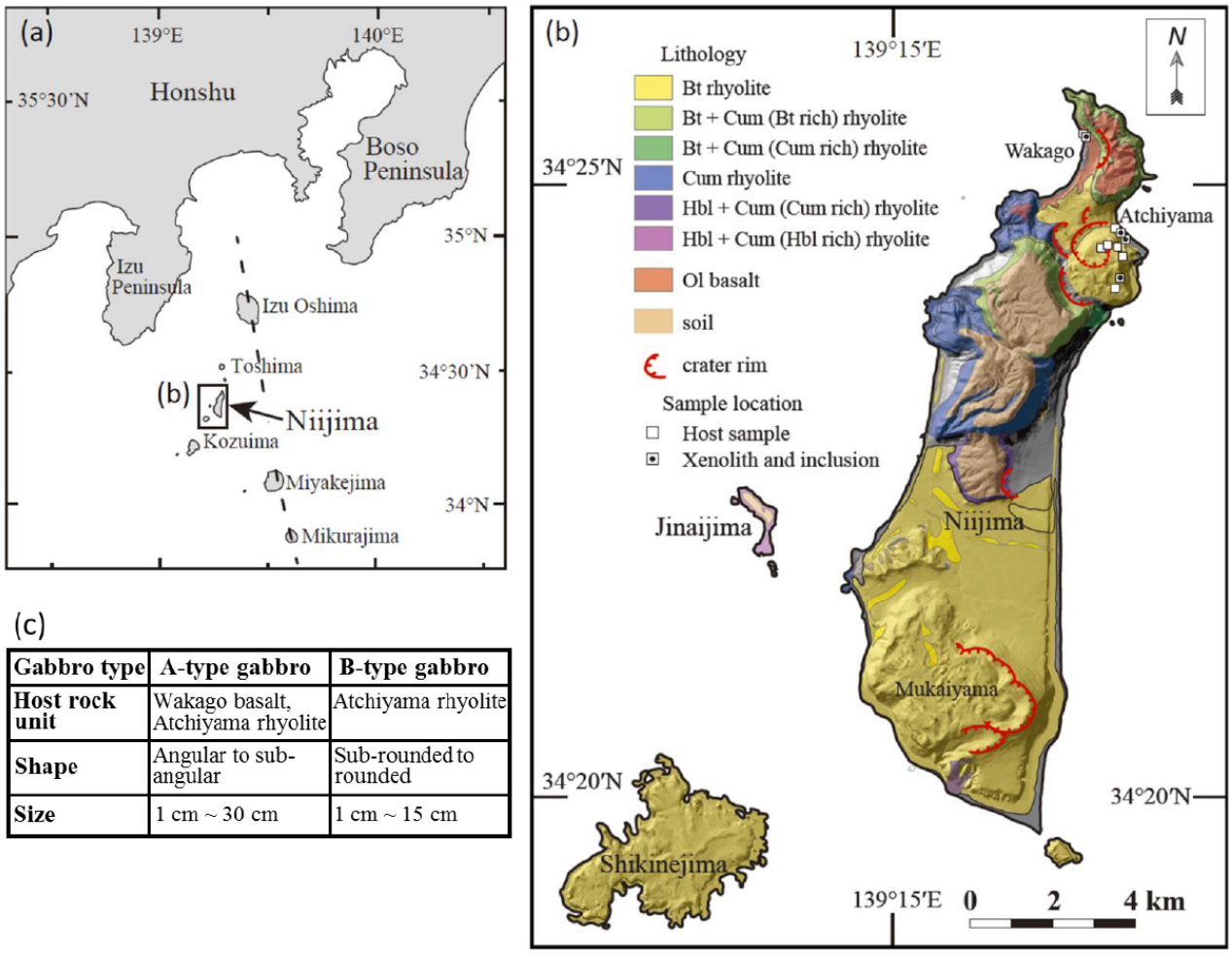

(c)

Gabbro type	A-type gabbro	B-type gabbro
Host rock unit	Wakago basalt, Atchiyama rhyolite	Atchiyama rhyolite
Shape	Angular to sub-angular	Sub-rounded to rounded
Size	1 cm ~ 30 cm	1 cm ~ 15 cm

Figure 1: (a) Tectonic setting of Niijima volcano in the northern Izu-Bonin arc. Dashed line marks the volcanic front of the northern Izu volcanic arc. (b) Simplified geological map of Niijima volcano showing sampling localities. Lithological classification is modified after Isshiki [16]. (c) Insert table showing the relationship between the gabbroic xenolith types and host rocks, and shape and size of xenoliths.

mas with the aim of understanding magmatic processes beneath Niijima volcano.

2 Geological background

Niijima volcano lies in the northern part of the Izu-Bonin arc about 20 km west of the volcanic front (Fig. 1a). Most of the frontal arc volcanoes in the arc produce basaltic magmas, but the Niijima volcano is composed mainly of monogenetic rhyolitic lava domes. Volcanism at Niijima probably started during the late Quaternary [16], and has produced at least 15 monogenetic, mostly rhyolitic eruptions [*e.g.* 16] (Fig. 1b). The rhyolitic volcanic episodes included three characteristic stages of lava production: a first stage of hypersthene-cummingtonite-hornblende rhyolite, a second stage of cummingtonite rhyolite, and a third stage of biotite rhyolite. Exceptions to this sequence were two eruptions of olivine-bearing basaltic magmas in the northern part of the island during the third stage. The first of these basaltic eruptions was in the Wakago area 2000 to 3000 years ago and the second was northwest of Atchiyama before the eruption that formed the Atchiyama lava dome [16, 18] (Fig. 1b). Andesite lavas are also in known at Niijima, but they are minor extent.

For this study, we collected samples of gabbroic xenoliths and their host rocks from the Atchiyama rhyolitic lava dome and from the Wakago basaltic pyroclastic deposit (Fig. 1b).

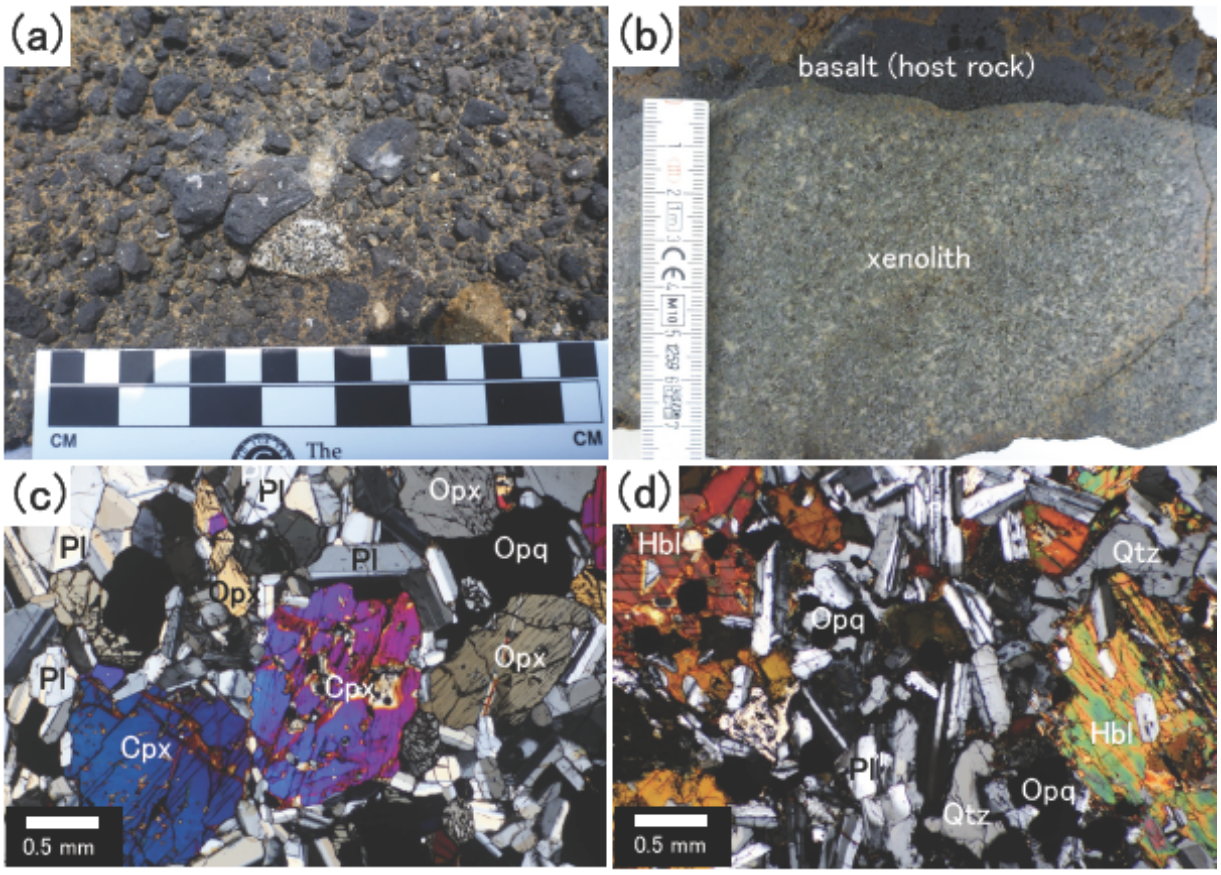

Figure 2: Photographs and photomicrographs of xenolith samples from Niijima volcano. (a) Photograph of an A-type gabbroic xenolith (center of image) in the Wakago pyroclastic deposit. (b) Photo of an A-type gabbro enclosed in the host basalt. (c) Photomicrograph of an A-type gabbro. (d) Photomicrograph of a B-type gabbro. Pl, plagioclase; Cpx, clinopyroxene; Opx, orthopyroxene; Hbl, hornblende; Qtz, quartz; Opq, opaque minerals.

3 Sample description and petrography

Gabbroic xenoliths are rare in the volcanic units at both Wakago and Atchiyama (Fig. 1c). Large angular xenoliths (up to 30 cm diameter) are found in the volcanic units, whereas the small xenoliths (1 to 15 cm in diameter) are rounded to sub-rounded (Figs. 2a and 2b). On the basis of rock textures and mineral associations, we identified two groups of xenoliths: amphibole-free gabbroic xenoliths (A-type gabbro) and amphibole-bearing gabbroic xenoliths (B-type gabbro). The A-type xenoliths correspond to the xenoliths of Azuma and Yashima [17] and are found in both the Wakago basaltic pyroclastic deposits and the Atchiyama rhyolitic lava dome (Figs. 1 and 2). The B-type xenoliths are found only in the Atchiyama rhyolitic lava dome. We collected non-altered xenolith samples in the outcrops. In small size of samples (5~7 cm), core parts of the xenoliths were selectively used for observations and chemical analyses, because the rim parts of the xenoliths sometimes were altered, or interacted in parts with surrounding volcanic rocks. Very small sizes of gabbro (< 5 cm) (mostly B-type) were excluded for observation and chemical analyses.

The A-type gabbro is a granular texture and its mineral assemblage is plagioclase, clinopyroxene, orthopyroxene, and Fe-Ti oxides with scarce olivine (Fig. 2c). Grain size ranges from 0.2 to 3 mm (average 1.0 mm). All of the samples contain various types and amounts of glasses. Most of the A-type gabbro has an adcumulate, even-grained mosaic texture [*e.g.* 19, 20]. Plagioclase, clinopyroxene, orthopyroxene, and magnetite are recognized as cumulus phases with unzoned post-cumulus overgrowth (Fig. 2c). Postcumulus interstitial magnetite is also present. However, narrowly zoned rims surrounding some crystals near their contact with patches of interstitial glass indicate mesocumulus growth. The B-type gabbros are clearly different from the A-type gabbros in both texture and modal mineralogy (Fig. 2d). Average grain size is less than 1 mm

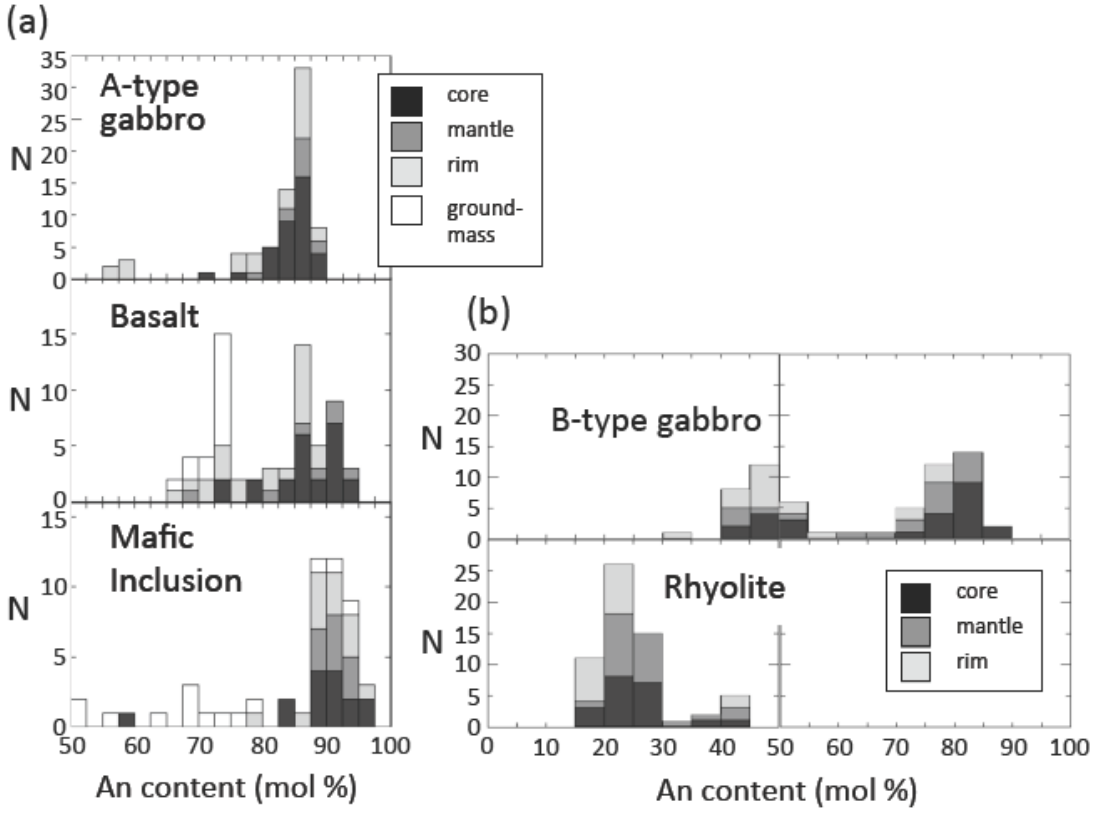

Figure 3: Histograms of anorthite (An) content of plagioclase in xenoliths and host volcanic rocks from Niijima volcano. (a) An content of plagioclase in the A-type gabbro, host basalt and mafic inclusion. (b) An content of plagioclase in the B-type gabbro and host rhyolite from Atchiyama volcano. An(%) = 100 × Ca/(Ca+Na) (atomic ratio). The An data are shown with division of core, mantle, rim, and groundmass plagioclase in the samples.

and the mineral assemblage is plagioclase, amphibole, quartz, Fe-Ti oxides, and rare minute clinopyroxene and orthopyroxene (Fig. 2d). The minerals are occasionally surrounded by unvesiculated interstitial glass. A peculiar feature is wide peripheral zonation in some plagioclases. This zoned rim is interpreted as the result of postcumulus crystallization in a closed system. The gabbroic cumulates of the B-type xenoliths are thus typical orthocumulates [*e.g.* 19, 21].

4 Analytical procedures

The chemical compositions of minerals from the gabbroic xenoliths and their host rocks were determined with an electron-microprobe analyzer (EPMA). Analyses were performed with an accelerating voltage of 15 kV and a probe current of 10 nA, and a beam diameter of 10 μm using JEOL-JXA 8530F (wavelength dispersive) electron probe microanalyzer at the Chemical Analysis Division the Research Facility Center for Science and Technology of the University of Tsukuba. The data were regressed using an oxide-ZAF correction program supplied by JEOL, using natural minerals and synthetic materials of known compositions as standards. All Fe reported as FeO.

Whole rock major and trace element compositions were determined with an inductively-coupled plasma mass spectrometer (ICP-MS) at Activation Laboratories Ltd. in Canada, and with an X-ray fluorescence (XRF) spectrometer (PANalytical MagiX PRO) at the Kitakyushu Museum of Natural History and Human History, Japan. For the XRF, the analytical methods presented in Mori and Mashima [22] were followed.

5 Results and discussion

The representative chemical compositions of minerals from the gabbroic xenoliths and their host rocks were shown in Table 1. The anorthite content (An = 100 × Ca/(Ca+Na)) of plagioclases in the A-type gabbro ranged from An_{56} to An_{90}; the most common composition was

Table 1: Representative chemical compositions of plagioclase, olivine, clinopyroxene, orthopyroxene and amphibole

Mineral	Plagioclase											
Type	A-type gabbro		B-type gabbro				Mafic inclusion		Basalt		Rhyolite[a]	
Sample	WGGAB-E1		AT-MI-02		Atx064a-03		AT908-2		A301-1		ATi909-2	
	c	r	c	r	c	r	c	gm	c	gm	c	r
SiO_2 (wt%)	46,33	46,49	47,53	49,63	46,46	54,21	45,63	53,06	46,10	50,58	63,87	65,39
TiO_2	0,00	0,03	0,00	0,03	0,01	0,07	0,00	0,03	0,00	0,02	0,01	0,00
Al_2O_3	32,97	32,74	33,01	31,59	33,99	28,67	33,96	29,25	33,92	30,62	22,45	21,79
Cr_2O_3	0,02	0,03	0,03	0,00	0,00	0,04	0,00	0,00	0,00	0,00	0,02	0,01
FeO(t)	0,54	0,47	0,57	0,55	0,58	0,45	0,58	0,68	0,71	1,11	0,12	0,07
NiO	0,00	0,01	0,01	0,00	0,00	0,02	0,00	0,00	0,02	0,00	0,00	0,01
MnO	0,01	0,01	0,00	0,00	0,00	0,04	0,03	0,00	0,00	0,05	0,06	0,02
MgO	0,02	0,03	0,06	0,00	0,07	0,05	0,03	0,09	0,10	0,19	0,02	0,01
CaO	17,60	17,27	17,18	15,45	17,33	11,33	18,92	13,15	17,93	14,56	5,13	3,91
Na_2O	1,45	1,62	1,75	2,62	1,66	5,11	0,84	4,06	1,33	3,02	8,66	9,31
K_2O	0,03	0,04	0,03	0,03	0,02	0,16	0,03	0,10	0,02	0,04	0,49	0,68
Total	98,98	98,74	100,16	99,91	100,13	100,13	100,00	100,42	100,13	100,19	100,84	101,19
	(O=8.00)											
Si	2,158	2,169	2,184	2,272	2,138	2,451	2,111	2,403	2,126	2,310	2,810	2,858
Ti	0,000	0,001	0,000	0,001	0,000	0,002	0,000	0,001	0,000	0,001	0,000	0,000
Al	1,810	1,800	1,787	1,705	1,844	1,528	1,852	1,561	1,844	1,649	1,164	1,122
Cr	0,001	0,001	0,001	0,000	0,000	0,001	0,000	0,000	0,000	0,000	0,001	0,000
Fe	0,021	0,018	0,022	0,021	0,022	0,017	0,022	0,026	0,028	0,042	0,004	0,003
Ni	0,000	0,000	0,000	0,000	0,000	0,001	0,000	0,000	0,001	0,000	0,000	0,000
Mn	0,001	0,000	0,000	0,000	0,000	0,002	0,001	0,000	0,000	0,002	0,002	0,001
Mg	0,001	0,002	0,004	0,000	0,005	0,003	0,002	0,006	0,007	0,013	0,001	0,000
Ca	0,878	0,863	0,846	0,758	0,855	0,549	0,938	0,638	0,886	0,713	0,242	0,183
Na	0,131	0,147	0,156	0,233	0,149	0,448	0,076	0,356	0,119	0,267	0,739	0,789
K	0,002	0,003	0,002	0,002	0,001	0,009	0,002	0,006	0,001	0,003	0,028	0,038
Total	5,003	5,005	5,001	4,992	5,014	5,010	5,002	4,997	5,012	4,999	4,991	4,995
An	87,00	85,46	84,47	76,53	85,20	55,08	92,55	64,17	88,15	72,74	24,65	18,84
Mg#												
Al^{IV}												
Al^{VI}												
Wo												
En												
Fs												

All Fe reported as FeO.

c, core; r, rim; gm, groundmass.

[a]: Rhyolite from Atchiyama lava dome, [b]: Rhyolite from Jinaijima lava dome. An: 100 × Ca/(Ca+Na) , Mg#: Mg/(Mg+Fe^{2+}), Wo :Ca/(Ca+Mg+Fe^{2+}), En: 100 × Mg/(Ca+Mg+Fe^{2+}), Fs: Fe^{2+}/(Ca+Mg+Fe^{2+}).

Al^{IV} and Al^{VI} calculated on a basis of cations per formula unit.

Continued on next page

Table 1: ... continued

Mineral	Olivine			Clinopyroxene			
Type	A-type gabbro	Mafic inclusion	Basalt	A-type gabbro	B-type gabbro	Mafic inclusion	Basalt
Sample	WGGAB-E1	AT908-2	A301-1	WG004-1-3	AT-MI-02	AT902-1	WA807-1h
	c	c	c	c	c	c	c
SiO_2 (wt%)	38,78	39,10	37,95	53,63	52,65	51,57	52,15
TiO_2	0,00	0,06	0,06	0,24	0,25	0,47	0,43
Al_2O_3	0,03	0,00	0,06	1,70	1,15	3,32	2,41
Cr_2O_3	0,06	0,02	0,00	0,04	0,02	0,00	0,01
FeO(t)	23,01	23,51	23,37	7,67	8,87	8,68	8,45
NiO	0,00	0,00	0,02	0,01	0,00	0,00	0,05
MnO	0,39	0,41	0,40	0,30	0,41	0,21	0,31
MgO	39,01	37,95	37,34	15,19	14,86	15,58	14,98
CaO	0,18	0,19	0,15	21,98	21,69	20,86	21,74
Na_2O	0,01	0,00	0,01	0,33	0,27	0,22	0,35
K_2O	0,00	0,02	0,00	0,01	0,00	0,00	0,01
Total	101,48	101,24	99,34	101,07	100,18	100,91	100,88
	(O=4.00)			(O=6.00)			
Si	0,997	1,008	1,000	1,964	1,960	1,899	1,925
Ti	0,001	0,001	0,001	0,006	0,007	0,013	0,012
Al	0,000	0,000	0,002	0,073	0,050	0,144	0,105
Cr	0,001	0,000	0,000	0,001	0,001	0,000	0,000
Fe	0,495	0,507	0,515	0,235	0,276	0,267	0,261
Ni	0,000	0,000	0,000	0,000	0,000	0,000	0,002
Mn	0,008	0,009	0,009	0,009	0,013	0,006	0,010
Mg	1,495	1,459	1,467	0,829	0,825	0,855	0,824
Ca	0,005	0,005	0,004	0,862	0,865	0,823	0,860
Na	0,001	0,000	0,000	0,023	0,019	0,015	0,025
K	0,000	0,001	0,000	0,000	0,000	0,000	0,000
Total	3,002	2,991	2,998	4,004	4,017	4,024	4,023
An							
Mg#	0,751	0,742	0,740	0,779	0,749	0,762	0,760
Al^{IV}				0,036	0,040	0,101	0,075
Al^{VI}				0,037	0,011	0,043	0,030
Wo				44,77	44,01	42,30	44,21
En				43,04	41,94	43,96	42,38
Fs				12,19	14,05	13,74	13,41

Continued on next page

Table 1: ...continued

Mineral	Orthopyroxene				Amphibole		
Type	A-type gabbro	B-type gabbro	Mafic inclusion	Basalt	B-type gabbro	Mafic inclusion	Rhyolite[b]
Sample	WG004-1-3 c	AT-MI-02 c	A312-2 c	WA807-1h c	AT-MI-02 c	AT902-1 gm	Jn1501-2 c
SiO_2 (wt%)	54,84	53,40	54,49	53,74	50,31	44,57	48,56
TiO_2	0,14	0,15	0,19	0,23	1,53	1,28	1,08
Al_2O_3	1,67	0,85	2,20	1,09	6,01	11,75	7,00
Cr_2O_3	0,00	0,04	0,00	0,00	0,02	0,00	0,00
FeO(t)	16,11	20,11	16,78	18,91	11,39	14,38	12,52
NiO	0,00	0,00	0,00	0,00	0,00	0,03	0,00
MnO	0,41	0,93	0,63	0,93	0,38	0,74	0,44
MgO	26,03	23,31	26,16	24,96	16,42	13,28	15,48
CaO	1,41	1,03	1,63	1,12	11,02	10,52	10,84
Na_2O	0,01	0,05	0,00	0,06	1,39	1,68	1,52
K_2O	0,00	0,00	0,00	0,02	0,14	0,13	0,17
Total	100,60	99,86	102,06	101,06	98,60	98,35	97,61
	(O=6.00)				(O=23.00)		
Si	1,971	1,977	1,941	1,983	7,181	6,517	7,058
Ti	0,004	0,004	0,005	0,005	0,164	0,141	0,118
Al	0,071	0,037	0,092	0,036	1,011	2,025	1,199
Cr	0,000	0,001	0,000	0,000	0,002	0,000	0,000
Fe	0,484	0,623	0,500	0,567	1,360	1,758	1,521
Ni	0,000	0,000	0,000	0,000	0,000	0,003	0,000
Mn	0,012	0,029	0,019	0,029	0,046	0,091	0,054
Mg	1,394	1,286	1,389	1,327	3,494	2,896	3,355
Ca	0,054	0,041	0,062	0,045	1,686	1,648	1,688
Na	0,000	0,004	0,000	0,001	0,385	0,475	0,428
K	0,000	0,000	0,000	0,000	0,025	0,025	0,031
Total	3,990	4,002	4,008	3,994	15,353	15,580	15,453
An							
Mg#	0,742	0,674	0,735	0,700	0,720	0,622	0,688
Al^{IV}	0,029	0,023	0,059	0,017	0,819	1,483	0,942
Al^{VI}	0,041	0,014	0,033	0,020	0,192	0,542	0,257
Wo	2,80	2,09	3,18	2,31			
En	72,14	65,97	71,20	68,42			
Fs	25,06	31,94	25,62	29,26			

Concluded

An_{80-90} (Fig. 3a). The cores and rims of most plagioclases in the A-type gabbro were similar compositions, consistent with adcumulus growth of the crystals. Some more sodic rims may represent postcumulus overgrowths in the mesocumulates. The core anorthite contents of plagioclases in the A-type gabbro are similar to those of the B-type gabbros, but were slightly lower than those in the host basalt (Wakago basalt) and mafic (basaltic) inclusions in the Atchiyama rhyolitic unit (Fig. 3a). The results suggest that plagioclase in the A-type gabbro might have precipitated from a slightly differentiated magma of the host basalt. In contrast, the anorthite content of plagioclases in the B-type gabbro showed a wider and bimodal compositional variation (An_{30-88}) with peaks at An_{40-55} and An_{70-88} (Fig. 3b). Although the highest anorthite content of plagioclase in B-type gabbro was similar to that of the A-type gabbro, the lower peak of anorthite content in the B-type gabbro was clearly lower than that of the A-type gabbro. The bimodal anorthite distribution of the B-type gabbro is very similar to that of andesite (of minor exposure in Niijima) representing mixing of basaltic and rhyolitic magmas [23]. The anorthite (An) contents of plagioclase from most of the B-type gabbros are higher than those in the host rhyolites (Fig. 3b). This result and the mineral assemblage of the B-type gabbros suggest that plagioclases in them were crystallized from intermediate (andesitic) magma, rather than rhyolitic magma.

The chemical compositions of olivine in the A-type gabbros showed a narrow range of Mg# (Mg# = $Mg/(Mg+Fe^{2+})$) values (0.73~0.76) and overlapped the compositions (Mg# = 0.67~0.77) of olivines in the host basalts (Table 1). Clinopyroxene from the A-type gabbro was calcic augite ($Wo_{42-45}En_{42-44}Fs_{11-13}$) (Wollastonite, Wo = 100 × $Ca/(Ca+Mg+Fe^{2+})$; Enstatite, En = 100 × $Mg/(Ca+Mg+Fe^{2+})$, Ferrosilite, Fs = 100 × $Fe^{2+}/(Ca+Mg+Fe^{2+})$), whereas that from the B-type gabbro ranged from augite to sub-calcic augite ($Wo_{37-44}En_{42-47}Fs_{13-16}$) (Table 1 and Fig. 4). Clinopyroxenes in the A-type gabbro had slightly higher Mg and Al contents than that in the B-type gabbro. The Al^{IV} content of clinopyroxene (calculated on the basis of cations per formula unit) in the A-type gabbro was 0.04-0.11, which was higher than that (0.01-0.05) in the B-type gabbro. The different Al^{IV} contents in clinopyroxene in both types of gabbro suggest a difference of crystallization pressures [*e.g.* 24, 25]. The compositional difference between cores and rims in orthopyroxenes was similar for both types of xenolith.

Amphiboles from the B-type gabbro were determined to be magnesiohornblende [26], characterized by higher Mg# and higher TiO_2 contents than those of amphibole from rhyolite (Table 1).

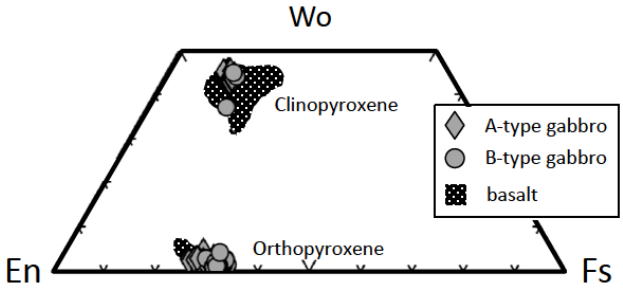

Figure 4: Pyroxene compositions for the two types of gabbroic xenoliths and volcanic rocks from Niijima volcano. Pyroxene compositions in the two types of gabbroic xenoliths and basalt from Niijima volcano are displayed on Enstatite-Ferrosilite-Wollastonite (En-Fs-Wo) ternary diagram. Pyroxene data ranges of host basalt are also included for comparison [32].

We calculated temperature and pressure conditions for the crystallization of the two types of gabbro under the assumption of crystallization at equilibrium within a magma chamber. Clinopyroxene-orthopyroxene pairs from the A-type gabbros yielded crystallization temperatures of 899 to 955°C, and pressures of 3.6 to 5.9 kbar using the method of geothermo- and geobarometry by Putirka [27]. The best results of these calculations were for mafic systems where the Mg# for clinopyroxene was > 0.75 [27]. For the B-type gabbro, the temperature was estimated using the amphibole-plagioclase thermometry by Holland and Blundy [28], and then based on the obtained temperature, pressure was calculated by the method of Anderson and Smith [29]. As a result, the B-type gabbro yielded crystallization temperatures of 687 to 824°C and pressures of 0.8 to 3.6 kbar.

Under silica-saturated conditions, the estimated temperature and pressure of crystallization for the B-type gabbros was 722 to 824°C at 0.8 to 2.3 kbar, whereas for a system under a silica-undersaturated, the estimates were 687 to 817°C at 1.0 to 3.6 kbar. Although the B-type gabbros contain interstitial quartz, it might represent a later stage of crystallization. Nevertheless, our results indicate that the A-type gabbros were derived from higher-temperature magmas and solidified at deeper levels than the B-type gabbros. These results (low pressure for B-type gabbro) are similar to those of Matsui *et al.* [30], who estimated the crystallization pressure for the biotite rhyolite to be 0.5-1.5 kbar.

For analyses of whole rock chemistry, we newly selected seven A-type gabbro and four B-type gabbro for chemical analyses. Also, some of the host basalt and rhyolite, andesite and mafic basaltic inclusions were deter-

Table 2: Representative whole rock major and trace element contents of two-types of gabbroic xenoliths, host basalt and rhyolite, and andesite and mafic inclusion in Niijima volcano

Type	A-type gabbro		B-type gabbro		Basalt	Mafic inclusion		Andesite	Rhyolite
Sample	WG004-1	WG Gab B	ATi907	Atx064a	WG004h	AT902 i	A312 b	R179	AT902 h
SiO_2 (wt%)	44,17	43,98	52,53	51,69	50,30	51,15	50,39	66,49	77,67
TiO_2	1,28	1,14	1,04	1,13	1,12	1,14	1,16	0,58	0,12
Al_2O_3	13,47	19,24	14,32	18,80	16,82	16,46	16,27	16,46	12,41
Fe_2O_3 (t)	17,91	14,52	16,58	11,08	13,35	13,67	13,80	4,56	1,01
MnO	0,20	0,15	0,26	0,20	0,21	0,21	0,21	0,18	0,06
MgO	7,98	5,54	5,08	4,64	5,02	4,88	4,78	1,25	0,16
CaO	12,66	14,81	6,62	9,60	10,19	10,23	10,15	5,14	0,98
Na_2O	1,12	1,32	3,75	2,59	2,36	2,53	2,34	4,36	4,29
K_2O	0,15	0,02	0,38	0,29	0,34	0,13	0,23	0,75	2,79
P_2O_5	0,06	0,04	0,05	0,10	0,14	0,09	0,10	0,20	0,03
LOI	0,37	0,07	0,17	0,24	0,32	0,41	0,39	0,51	0,71
Total	99,37	100,80	100,80	100,40	100,20	100,90	99,80	100,50	100,20
(ppm)									
Sc	62	50	56	35	45	49	49	17	4
Be	< 1	< 1	< 1	< 1	< 1	< 1	< 1	< 1	1
V	820	691	642	405	440	497	494	56	11
Cr	< 20	50	< 20	< 20	< 20	< 20	< 20	< 20	< 20
Co	53	31	29	28	36	27	32	4	< 1
Ni	40	< 20	< 20	< 20	< 20	< 20	< 20	< 20	< 20
Cu	340	20	< 10	40	80	80	30	< 10	< 10
Zn	80	70	130	70	110	90	100	90	< 30
Ga	16	18	16	18	18	17	17	16	12
Ge	1,7	1,6	2,1	2,2	2,2	1,9	2,2	2,0	2,3
As	< 5	< 5	< 5	< 5	< 5	< 5	< 5	< 5	< 5
Rb	< 1	< 1	5	5	5	< 1	4	10	55
Sr	224	338	136	314	270	245	245	274	77
Y	12,9	7,5	15,2	14,7	17,5	15,4	16,4	29,1	20,0
Zr	24	14	28	47	46	37	39	103	67
Nb	0,2	12,1	2,4	1,6	2,0	2,4	2,7	2,7	5,6
Mo	< 2	< 2	< 2	< 2	< 2	< 2	< 2	< 2	< 2
Ag	< 0.5	< 0.5	< 0.5	0,8	< 0.5	< 0.5	< 0.5	0,7	< 0.5
In	< 0.1	< 0.1	< 0.1	< 0.1	< 0.1	< 0.1	< 0.1	< 0.1	< 0.1
Sn	< 1	< 1	< 1	1	< 1	7	< 1	< 1	1
Sb	< 0.2	< 0.2	< 0.2	< 0.2	< 0.2	< 0.2	< 0.2	< 0.2	< 0.2
Cs	< 0.1	< 0.1	0,1	0,3	0,3	< 0.1	0,3	0,6	1,9
Ba	32	21	58	85	85	84	93	208	564
La	1,20	1,18	1,36	3,78	3,64	3,08	2,73	6,74	15,50
Ce	4,30	3,21	3,85	9,38	9,49	7,97	6,98	17,20	30,80
Pr	0,70	0,52	0,69	1,42	1,54	1,16	1,14	2,60	3,79
Nd	4,01	2,75	3,87	7,03	7,85	5,64	5,95	13,20	14,20
Sm	1,36	0,93	1,52	2,00	2,30	1,85	2,03	3,66	2,88
Eu	0,523	0,480	0,656	0,807	0,944	0,802	0,857	1,310	0,487
Gd	1,91	1,30	2,19	2,18	3,00	2,46	2,74	4,32	2,92
Tb	0,36	0,23	0,42	0,40	0,54	0,46	0,50	0,81	0,54
Dy	2,30	1,38	2,92	2,58	3,23	2,94	3,13	5,12	3,30
Ho	0,47	0,28	0,61	0,53	0,65	0,59	0,64	1,04	0,68
Er	1,37	0,85	1,83	1,61	2,03	1,84	1,92	3,14	2,17
Tm	0,207	0,130	0,291	0,248	0,319	0,284	0,308	0,518	0,374
Yb	1,37	0,87	1,94	1,65	2,04	1,84	2,04	3,53	2,71
Lu	0,218	0,131	0,294	0,237	0,286	0,276	0,288	0,549	0,423
Hf	0,7	0,6	1,0	1,1	1,3	1,0	1,1	2,7	2,1
Ta	< 0.01	0,18	0,05	0,04	0,03	0,05	0,13	0,10	0,52
W	< 0.5	< 0.5	< 0.5	< 0.5	< 0.5	< 0.5	< 0.5	< 0.5	< 0.5
Tl	< 0.05	0,31	< 0.05	0,31	0,05	< 0.05	< 0.05	0,09	0,29
Pb	< 5	< 5	< 5	< 5	< 5	< 5	< 5	< 5	6
Bi	< 0.1	< 0.1	< 0.1	< 0.1	< 0.1	< 0.1	< 0.1	0,1	0,3
Th	0,12	0,40	0,20	0,37	0,42	0,40	0,36	0,78	3,81
U	0,06	0,06	0,10	0,14	0,17	0,12	0,17	0,42	1,41

The data in the table are selected data by ICP-MS determination, and the data by XRF are included in the Fig. 5.

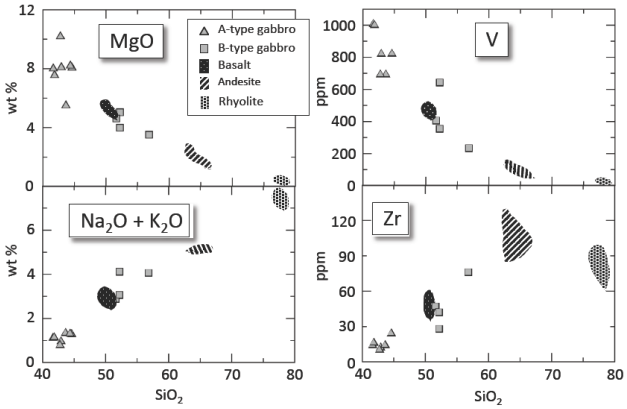

Figure 5: Comparison of selected major and trace elements for the two types of gabbro and host rocks from Niijima volcano. Andesite data from Shimawakezawa pyroclastic unit and some data of the basaltic mafic inclusions are from the Atchiyama rhyolite from Endo [23]. Some of the basalt and andesite data are used from Isshiki [16].

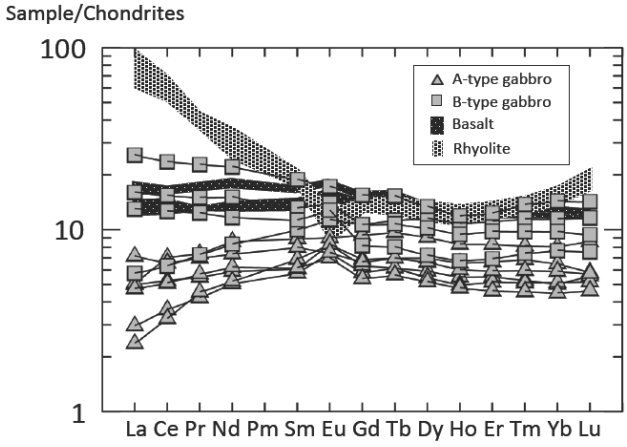

Figure 6: Rare earth element (REE) variation diagrams for xenoliths and volcanic rocks from Niijima volcano. REE data were normalized to C1 chondrite [33]. Basaltic inclusion data from Atchiyama rhyolite are nearly the same with basalt data in Wakago. Most of the data of rhyolites in Niijima are referred from [23, 32] and shown (light-shaded area).

mined for comparison. Whole rock chemistry data (Table 2) show that the SiO_2 contents (wt. %) of the A- and the B-type gabbros are 42 to 45 % and 51 to 57 %, respectively (Fig. 5). MgO contents were 5.5-10.3 % for the A-type and 3.8-5.1 % for the B-type gabbro. V and Zr contents also differ among the two types of gabbro, and their host rocks, and minor andesite units (Fig. 5), and each of these, with the exception of the rhyolite, shows a degree of linearity.

Chondrite-normalized rare earth element (REE) patterns of the A-type gabbros (Fig. 6) are characterized by depletion of light rare-earth elements (LREEs) pattern, and a minor positive Eu anomaly, which together suggest the accumulation of plagioclase. In contrast, the REE patterns of the B-type gabbros have a flatter pattern, with only slight depletion of LREEs. A weak positive Eu anomaly is also apparent for B-type gabbros. The REE patterns of the B-type gabbros clearly differ from those of the host rhyolites, which have much higher LREE contents (Fig. 6). It is possibly assumed that the B-type gabbro was formed from andesitic host magma, but not from basaltic and rhyolitic. Considering mineral assemblages and chemistries, the whole rock chemistry for the two types of gabbro and their host rocks supports crystallization of the A-type gabbro from a mafic (basaltic) magma and the B-type gabbro from a mafic to intermediate (andesitic composition) magma.

These results are concordant with our petrographic results and provide strong evidence that both types of gabbro represent cumulates removed from parental magmas during crystallization and fractionation. Whole rock chemistry suggests that the A-type gabbro was derived from a basaltic parental magma similar to that erupted at Wakago, and that the B-type gabbro was not derived directly from either the basaltic or rhyolitic magmas that host the xenoliths, although it is possible that the parental magma of the B-type gabbro was a fractionation product of the basaltic magma. Our results (especially mineral assemblages and mineral chemistries) suggest that an intermediate (andesitic) magma was the parental magma for the B-type gabbro.

Similar results have been reported for xenoliths of cumulate gabbro elsewhere, including dacite erupted at Mount St. Helens (Washington) from 1980 to 1983 [*e.g.* 14]. Several types of gabbro-norite cumulates have been interpreted to be derived from mafic plutons formed by multiple emplacements of basaltic magma at middle to upper crustal levels beneath a volcano. Gabbroic cumulates within rhyolites at Little Glass Mountain (California) have been interpreted to represent a two-stage fractionation model on the basis of compositional gaps in plagioclase zoning in the rhyolite [15]. These studies of cumulate gabbro in felsic (dacite-rhyolite) volcanic products strongly suggest that complex processes of magma intrusion and crystal-fractionation involving parental magma with various compositions have occurred at relatively in shallow crustal levels beneath volcanoes.

The evolution of magmatic system in Niijima volcano inferred from the stratigraphic succession of lavas [16, 30] is consistent with the development of fractionated lavas by open-system magmatic processes. Identification of the cumulate from which mafic xenoliths originated may prove that crystal fractionation has played a significant role in the evolution of the magmatic system. It is likely that

these mafic xenoliths are products of liquid that was cognate with the effusive basalt and andesite. It is therefore probable that an ultramafic cumulate residuum remains in the middle-lower crust beneath the volcanic edifice, its presence is consistent with crustal structure modeled on the basis of seismic profiles [*e.g.* 31]. Therefore, the petrographical and chemical characteristics, and their assumed crystallization processes of gabbroic xenoliths at the rhyolite dominated Niijima volcano suggest that the existence of various cumulate bodies at different levels beneath the volcano, and that the effect of mafic to intermediate magmas beneath rhyolitic volcanoes can have considerable influence on the erupted products of these volcanoes.

6 Conclusions

Two different types of gabbroic xenoliths (A- and B-type xenoliths) in volcanic products among the rhyolite dominated Niijima volcano, northern Izu-Bonin volcanic arc (central Japan) were investigated on the basis of petrography, petrology and geochemistry. A-type gabbroic xenoliths consisting of plagioclase, clinopyroxene, and orthopyroxene with an adcumulate texture were found in both basalt and rhyolite units, and B-type gabbroic xenoliths consisting of plagioclase and amphibole with an orthocumulate texture were found only in rhyolite unit. The A-type gabbro were estimated to have formed at higher temperatures (899-955°C) and pressures (3.6-5.9 kbar) than the B-type gabbro (687-824°C and 0.8-3.6 kbar). These calculation modelling, and mineral and whole-rock chemistries suggest different parental magmas for the two types of gabbro. The A-type gabbro was assumed to have been produced from basaltic magma, whereas the B-type gabbro was formed from an intermediate (andesitic) magma. The results for the gabbroic xenoliths in the Niijima volcano indicate that mafic to intermediate cumulate bodies of different origins and some different fractionation processes existed beneath the rhyolite dominated volcano.

Acknowledgement: We are grateful to N. Nishida and N. Chino for their kind helps in microprobe analyses. We thank A. Takada at the Geological Survey of Japan and T. Tsunogae at the University of Tsukuba for their fruitful comments and discussions. We deeply acknowledge to two anonymous reviewers and Dr. J. Barabach, (Managing Editor) for their critical comments and advices that significantly improved our manuscript.

References

[1] Bacon C.R., Metz J., Magmatic inclusions in rhyolites, contaminated basalts, and compositional zonation beneath the Coso volcanic field, California. Contrib. Mineral. Petrol., 1984, 85, 346-365.

[2] Beard J.S., Characteristic mineralogy of arc-related cumulate gabbros: implications for the tectonic setting of gabbroic plutons and for andesite genesis. Geology, 1986, 14, 848-851.

[3] Hickey-Vargas R., Abdollahi M.J., Parada M.A., López-Escobar L., Frey F.A., Crustal xenoliths from Calbuco volcano, Andean Southern Volcanic Zone: implications for crustal composition and magma-crust interaction. Contrib. Mineral. Petrol., 1995, 119, 331-344.

[4] Brown S.J.A., Burt R.M., Cole J.W., Krippner S.J.P., Price R.C., Cartwright I., Plutonic lithics in ignimbrites of Taupo Volcanic Zone, New Zealand; sources and conditions of crystallisation. Chem. Geol., 1998, 148, 21-41.

[5] Costa F., Dungan M.A., Singer B.S., Hornblende- and phlogopite-bearing gabbroic xenoliths from Volcán San Pedro (36° S), Chilean Andes: evidence for melt and fluid migration and reactions in subduction-related plutons. J. Petrol., 2002, 43(2), 219-241.

[6] Coulon C., Clocchiatti R., Maury R.C., Westercamp D., Petrology of basaltic xenoliths in andesitic to dacitic host lavas from Martinique (Lesser Antilles): evidence for magma mixing. Bull. Volcanol., 1984, 47(4), 705-734.

[7] Koyaguchi T., Evidence for two-stage mixing in magmatic inclusions and rhyolitic lava domes on Niijima Island, Japan. J. Volcanol. Geotherm. Res., 1986, 29, 71-98.

[8] Aoki K., Petrology of mafic inclusions from Itinome-gata, Japan. Contrib. Mineral. Petrol., 1971, 30, 314-331.

[9] Shimazu M., Kawano Y., Kaji K., Igarashi S., Chemical compositions and Sr, Nd isotope ratios of gabbroic xenoliths in calc-alkali andesites of Naeba and Torikabuto volcanoes, North Fossa Magna, central Japan. J. Mineral. Petrol. Econ. Geol., 1991, 86, 53-64.

[10] Aoki K., Kuno H., Gabbro-quartz diorite inclusions from Izu-Hakone region, Japan. Bull. Volcanol., 1972, 36(1),164-173.

[11] Arculus R.J., Wills K.J.A., The petrology of plutonic blocks and inclusions from the Lesser Antilles island arc. J. Petrol., 1980, 21(4), 743-799.

[12] Yasui M., Togashi S., Shimomura Y., Sakamoto S., Miyaji N., Endo, K., Petrological features and origin of the gabbroic fragments contained in the 1707 pyroclastic fall deposits, Fuji Volcano. Bull. Volcanol. Soc. Japan, 1998, 43(2), 43-59 (in Japanese with English abstract).

[13] Pallister J.S., Hoblitt R.P., Crandell D.R., Mullineaux D.R., Mount St Helens a decade after the 1980 eruptions: magmatic models, chemical cycles, and a revised hazards assessment. Bull. Volcanol., 1992, 54, 126-146.

[14] Heliker C., Inclusions in Mount St. Helens dacite erupted from 1980 through 1983. J. Volcanol. Geotherm. Res., 1995, 66, 115-135.

[15] Brophy J.G., Dorais M.J., Donnelly-Nolan J., Singer B.S., Plagioclase zonation styles in hornblende gabbro inclusions from Little Glass Mountain, Medicine Lake volcano, California: implications for fractionation mechanisms and the formation of composition gaps. Contrib. Mineral. Petrol., 1996, 126, 121-136.

[16] Isshiki N., Geology of the Nii Jima district. With Geological Sheet Map at 1:50,000, Geological Survey of Japan, Tsukuba, Japan, 1987 (in Japanese with English abstract).

[17] Azuma K., Yashima R., A leucocratic xenolith from Niizima, Izu. Science Reports of the Faculty of Edu. Fukushima Univ., 1984, 34, 25-27 (in Japanese with English abstract).

[18] Tsukui M., Saito K., Hayashi K., Frequent and intensive eruptions in the 9th century, Izu Islands, Japan: Revision of volcanostratigraphy based on tephras and historical document. Bull. Volcanol. Soc. Japan., 2006, 51(5), 327–338 (in Japanese with English abstract).

[19] Wager L.R., Brown G.M., Wadsworth W.J., Types of igneous cumulates. J. Petrol., 1960, 1(1), 73-85.

[20] Tollan P.M.E., Bindeman I., Blundy J.D., Cumulate xenoliths from St. Vincent, Lesser Antilles Island Arc: a window into upper crustal differentiation of mantle-derived basalts. Contrib. Mineral. Petrol., 2012, 163, 189– 208.

[21] Jeffery A.J., Gertisser R., Troll V.R., Jolis E.M., Dahren B., Harris C., Tindle A.G., Preece K., O'Driscoll B., Humaida H., Chadwick J.P., The pre-eruptive magma plumbing system of the 2007–2008 dome-forming eruption of Kelut volcano, East Java, Indonesia. Contrib. Mineral. Petrol., 2013, 166, 275–308.

[22] Mori Y., Mashima H., X-ray fluorescence analysis of major and trace elements in silicate rocks using 1:5 dilution glass beads. Bulletin of the Kitakyushu Museum of Natural History and Human History, 2005, Ser A (3), 1–12.

[23] Endo D., Petrological and petrochemical characteristics of the volcanic products in the Niijima volcano, northern Izu-Ogasawara arc. Master thesis, University of Tsukuba, Japan, 2012.

[24] Aoki K., Kushiro I., Some clinopyroxenes from ultramafic inclusions in Dreiser Weiher, Eifel. Contrib. Mineral. Petrol., 1968, 18, 326-337.

[25] Jankovics M.É., Dobosi G., Embey-Isztin A., Kiss B., Sági T., Harangi S., Ntaflos T., Origin and ascent history of unusually crystal-rich alkaline basaltic magmas from the western Pannonian Basin. Bull. Volcanol., 2013, 75, 749, doi:10.1007/s00445-013-0749-7

[26] Leake B.E., Woolley A.R., Arps C.E.S., Birch W.D., Gilbert M.C., Grice J.D., Hawthorne F.C., Kato A., Kisch H.J., Krivovichev V.G., Linthout K., Laird J., Mandarino J.A., Maresch W.V., Nickel E.H., Rock N.M.S., Schumacher J.C., Smith D.C., Stephenson N.C.N., Ungaretti L., Whittaker E.J.W., Youzhi G., Nomenclature of amphiboles: Report of the Subcommittee on Amphiboles of the International Mineralogical Association, Commission on New Minerals and Mineral Names. Can. Mineral., 1997, 35, 219-246.

[27] Putirka K.D., Thermometers and barometers for volcanic systems. In: Putirka K.D., Tepley F.J. (Eds.), Minerals, Inclusions and Volcanic Processes, Reviews Mineral. Geochem 69. Mineralogical Society of America, Washington, D.C., 2008, 61-120.

[28] Holland T., Blundy J., Non-ideal interactions in calcic amphiboles and their bearing on amphibole- plagioclase thermometry. Contrib. Mineral. Petrol., 1994, 116, 433-447.

[29] Anderson J.L., Smith D.R., The effects of temperature and fO_2 on the Al-in-hornblende barometer. Am. Mineral., 1995, 80, 549-559.

[30] Matsui R., Nakamura M., Yoshiki K., Kuritani T., Yoshida T., Suzuki Y., Nagahashi Y., A petrological study on the magma plumbing systems in the Niijima and Shikinejima volcanoes, Izu Islands. Abstracts of Japan Geoscience Union Meeting, Makuhari, Japan, 2009, V160-P005.

[31] Kodaira S., Sato T., Takahashi N., Ito A., Tamura Y., Tatsumi Y., Kaneda Y., Seismological evidence for variable growth of crust along the Izu intraoceanic arc. J. Geophys. Res., 2007, 112, B05104, doi:10.1029/2006JB004593

[32] Endo D., Arakawa Y., Ikehata K., Oshika J., Shinmura T., Mori Y., Two types of gabbroic xenoliths from Niijima volcano, Izu-Bonin arc: petrological and geochemical constraints. Abstracts of Annual Meeting of Japan Association of Mineralogical Sciences, Kumamoto, Japan, 2014, R7-08.

[33] Sun S.S., McDonough W.F., Chemical and isotopic systematics of oceanic basalts: Implications for mantle composition and processes. In: Saunders A.D., Norry M.J. (Eds.), Magmatism in the Ocean Basins, Geological Society, London, Special Publications, 1989, 42, 313–345.